

Flow Induced Vibration in Pump Impellers: A Case Study

Samuel J. Brown

Quest Engineering and Development Corporation, Humble, TX USA

INTRODUCTION

Although the phenomenon of flow induced vibration has been studied for a number of decades, only more recently has it been studied with respect to pressure systems design. In fact, because of the complex nature of flow-induced vibration (FIV), it has led prominent researchers in the field to conclude that it is extremely important to understand the flow-induced vibration mechanism in order to "design out of the problem" (DOP), rather than to attempt to design the problem area on the basis of analysis with a high degree of certitude, (i.e., predicting system response). Designing out of the problem is no easy task and may not be affected by addressing one parameter but rather several: structural contour, material selection, flow properties, structural stiffness, damping, and fluid-structure coupling.

In this paper the mechanism of flow induced vibration fatigue failure of large circulating water pumps is discussed. This paper provides an overview of the inter-relationship of finite element and theoretical analysis, component and material testing, operational data, fabrication, and repair practices.

BACKGROUND AND THE NATURE OF THE PROBLEM

Prompted by a number of blade failures of circulating water pump (CWP) impellers, fabricated of Nickel Aluminum Bronze (NiAlBz) and 304L stainless steel, an analytical program was undertaken to identify the mode and mechanism of failure. Figure 1 illustrates the characteristic failure observed in all impeller blades in which crack initiation began at the blade to hub leading edge and grew on an approximate 45 degree angle to the hub tangent radially outward. Figure 2 provides a cross section of the impeller, in which the average blade thickness is approximately 7/8 of an inch and the hub varies from 1.75 to approximately 2.25 inches (adjacent to the shaft attachment). The NiAlBz impellers operated approximately 8 years before severe blade cracking failure; and the 304L stainless steel impeller failed within a year. In the case of the 304L impellers, fatigue cracking was exacerbated by the presence of chlorides in the circulating water and the attempt to perform field welds on the initiated cracks. A discussion of the problems associated with the use of 304L stainless steel in large impeller-propeller castings and weld repairs is discussed by Klein (1981) and will not be discussed in

any further detail in this paper.

Some examples of previously reported similar FIV problems are reported by Parmakian and Jacobson (1952), Gongwer (1952), and Donaldson (1958), for hydraulic turbines and marine propellers.

TEST DATA

As a part of this study, insitu vibrational response (displacements vs. time) was recorded for a number of NiAlBz and 304L stainless steel impellers. A total of 4 NiAlBz and 4 304L stainless steel impellers were observed to fail as shown in Figure 1. In the one second time vs. displacement plot shown in Figure 3, it can be seen that the predominant modes of vibration occurred at approximately 4.6 HZ and 69 HZ. A sampling of the insitu operational data indicates that the two predominant frequencies for all impellers range from 4.6 to 5.1 HZ for the largest response and 59 to 69 HZ for the second dominant vibrational response.

The laboratory determined natural frequencies of the NiAlBz and 304L stainless steel impellers in air were found to be relatively close: mode 1 is 114 to 120 HZ, mode 2 is 135 to 140 HZ, and mode 3 is 250 to 282 HZ (note the impeller was placed on the lab floor while it was "rung" or "plucked"). A mapping of the experimentally determined modes with a comparison to the mode shapes obtained by finite element analysis gives one a better picture of the relationship of the local and global modes of vibration with the corresponding frequencies, which will be discussed briefly in the next section.

Finally, fatigue tests utilizing impeller samples were performed and are illustrated in Figure 4. Note that the tested NiAlBz fatigue properties has better performance (on an order of magnitude on cycles) than the 304L stainless steel.

THEORETICAL ANALYSIS

Figure 5 illustrates a finite element representation of the CWP impellers. The finite element model consists of 720 corner nodes, 660 elements and 6 degrees of freedom. The finite element method is well known and discussed in reference texts such as those of Zienkiewicz (1977). The finite element model is supported in the annular region (shaft-hub attachment) "D" (see Figure 5). Figures 6 and 7 show the pendulum and $n=2$ mode of the impeller respectively. Note the convention for mode shape is the same as that used for a circular cylinder in Brown (1982). The impeller natural frequencies in air are tabulated in Table 1. Item 1 in Table 1 indicates the natural frequencies in air of the impeller for $n=2$ and the pendulum mode. Items 3 and 4 in Table 1 illustrate that weld reinforcement or contouring do not significantly alter the natural frequencies of the impeller's first three modes. Item 5 indicates that the natural frequency of the impeller blade on a stiffened shell is relatively high (approximately 281 HZ) which coincides closely to the 3rd mode determined in the experimental tests in air. Item 6 in Table 1 illustrates that the frequencies of the impeller cone or hub without blades strongly influence the natural frequencies of the impeller system with blades and hub - Item 1.

Next, the natural frequency of the impeller in water (Item 2,

Table 1) is determined by using the finite element fluid-structure model coupling techniques discussed by Brown (1978) and (1983) and the virtual mass simplified formula techniques outlined by Brown (1982).

Table 1, Item 7 lists a number of excitation frequencies of concern; f_s - the rotational frequency of 4.54 HZ, f_B - the blade passing frequency of 22.7 HZ, and f_v - the flow induced vibration frequencies due to vortex shedding at the free end of the blade and at the root of the blade. The f_v values in Table 1, Item 7 are based on the formulas developed by Gongwer (1952);

$$f_v = \frac{SV}{d'} \quad (1)$$

where corrected thickness:

$$d' = d + d^* \quad (2)$$

and the virtual thickness addition is:

$$d^* = 0.0297 \left[\frac{L}{\left(\frac{VL}{v}\right)^{1/5}} \right] \quad (3)$$

in which: f = vortex shedding frequency (hertz)
 S = Strouhal number (=0.18, according to Gongwer's (1952))
 V = flow velocity
 d = blade thickness at trailing edge
 L = blade length
 v = kinematic viscosity of fluid

The above formula is based on experiments with semicircular trailing edges (Figure 8b), and constant trailing edge thickness.

Edge shape can be an important factor in controlling the vortex shedding frequency as discussed by Donaldson (1956), Heskestad and Olberts (1980), Toebes (1981), Wood (1971), and Greenway (1973). Resonant frequencies occur not only when structural and vortex frequencies are coincident but when they are close (synchronization or "lock-in") and some of these factors are discussed by Blevins (1977), Chen (1985) and King (1973).

CONCLUSIONS

In this example case, the analysis shows that natural frequency detuning of the structure is more affected by geometrical changes in the cone than in the blades. In addition other options to affect the performance of the impeller are: 1) change the vortex shedding frequency (by changing the trailing edge as shown in Figure 8(d or e), 2) reduce vortex strength, or 3) increase the fatigue strength of the blades (for example utilizing a duplex stainless steel).

This paper illustrates: 1) that flow induced vibration is a complex mechanism of vibration but notes the importance of starting with basic analysis methods, 2) the need to correlate various system needs such as equipment performance, structure performance, functional performance, and load mechanisms, 3) the need to identify potential problem areas in the early stages of design and screen or prioritize them. Base prioritization on DOP detune, test, and insitu monitoring by planning to perform analysis, lab or model test, insitu test or pre-operational test, monitoring for data, and preventive

maintenance, and 4) retrofit, modify, or replace based upon analysis and input data from field test or operation as required.

Finally, the efforts of QED, Standard Alloy, and Intertech Services Inc. and (particularly C. Sundararajan and T. J. Brown) as well as numerous others are acknowledged.

REFERENCES

- Blevins, R.D.(1977). Flow Induced Vibration. VanNostrand Reinhold
 Brown, S. J., Hsu, K. H. (1978). On the use of the Finite Element Displacement Method to Solve Solid-Fluid Interaction Vibration Problems. Fluid Transients and Acoustics in the Power Industry (ASME), N.Y.
 Brown, S. J., (1982). Hydro-dynamic Response of Fluid Coupled Cylinders: Simplified Damping and Inertia Coefficients. Welding Research Bulliten, No. 281 - Oct.
 Brown, S. J., Chu, M. (1983). Case Study of the Seismic Response of Fluid-Coupled Flexible Cylinders. Journal of Experimental Mechanics. Sept.
 Chen, S. S., (1985). Flow Induced Vibration of Cylindrical Structures. U. S. Department of Energy, Argonne National Laboratory (ANS 85-51). Jun.
 Donaldson, M., (1956). ASME Transactions. Jul.
 Gongwer, C. A., (1952). Journal of Applied Mechanics. Dec.
 Greenway, M. E., Wood, C. J., (1973). Journal of Fluid Mech.
 Heskestad, G., Olberts, D. R., (1960). J. Engrn. Powere. Apr.
 King, R., Prosser, M. J., (1973). J. Sound and Vibration.
 Klein, J. L., (1981). Repair of Stainless Steel and Bronze Propellers: Theory and Practice. American Welding Society, Welding in Shipbuilding. Conference Proceedings, Mar.
 Parmakian, J., Jacobson, R. S., (1952). ASME Transactions, Jul.
 Toebes, G. H., Eagelson, P. S., (1961). J. Basic Engrn. Dec.
 Wood, C. J., (1971). Journal of Sound and Vibration.
 Zienkiewicz, O. C.,(1977). The Finite Element Method. McGraw-Hill

TABLE 1

FREQUENCY IN HZ (MODE OF CONE - (B, m, n))

	f1	f2	f3
#1	Cone & blades in air		
	161(2)	162(2)	173(P =pendulum)
#2	Cone & blades in water		
	73(2)	74(2)	61.3(P=(1,0,0))
#3	Cone & blades (stiffened w/o mass @ root) in air		
	180(2)	182(2)	235(P)
#4	Cone & blades (stiffened w/ added mass @ root) in air		
	170(2)	171(2)	227(P)
#5	Blade only in air		
	281(NA)	309(NA)	335(NA)
#6	Cone in air		
	115(2)	151(P)	211(3=(0,0,3))
#7	Excitation Frequencies		
	f_e = Rotational frequency = 4.54HZ		
	f_B = Blade passing frequency = 22.7HZ		
	= RPM x no blades		
	60		
	$79 \leq f_v$ (free end) ≤ 149 HZ		} Flow Induced Vibration
	$34 \leq f_v$ (root) ≤ 63.3 HZ		

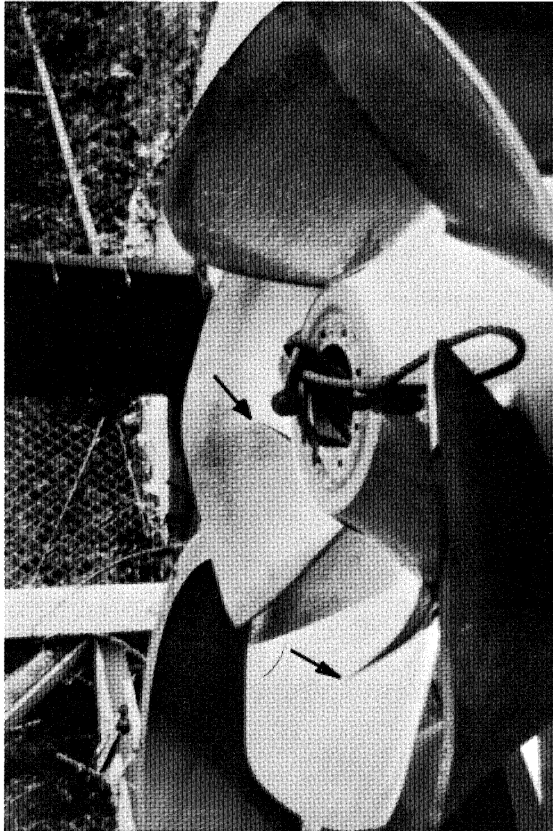


FIG 1. IMPELLER BLADE CRACKS (AT ROOT)

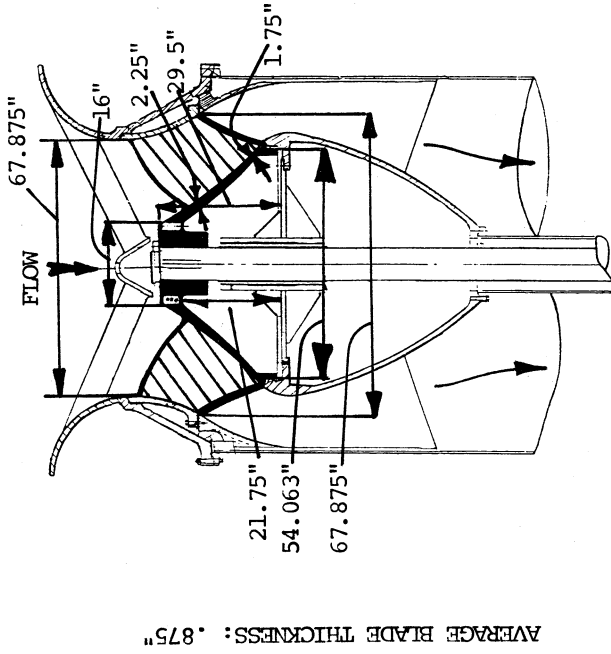


FIG 2. CROSS SECTION OF IMPELLER IN PUMP CASE

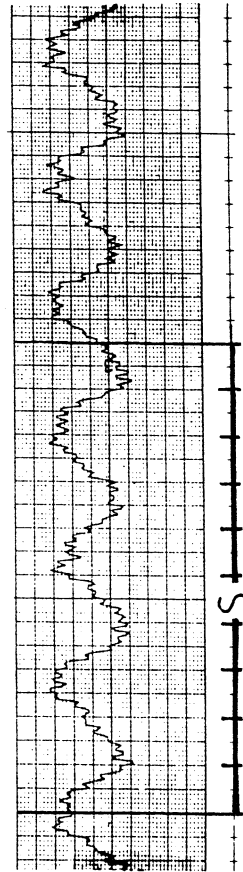


FIG 3. DISPLACEMENT RESPONSE VS. TIME AT IMPELLER SHAFT

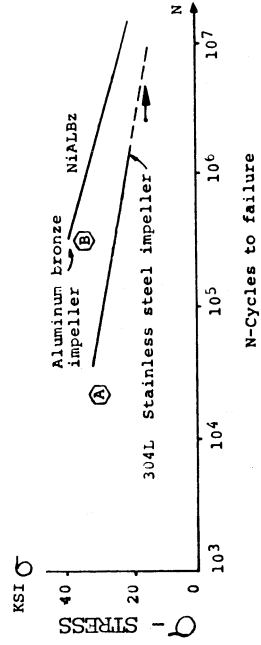


FIG 4. RESULTS OF THE ROTATING BEAM FATIGUE TESTS FROM IMPELLER SPECIMEN

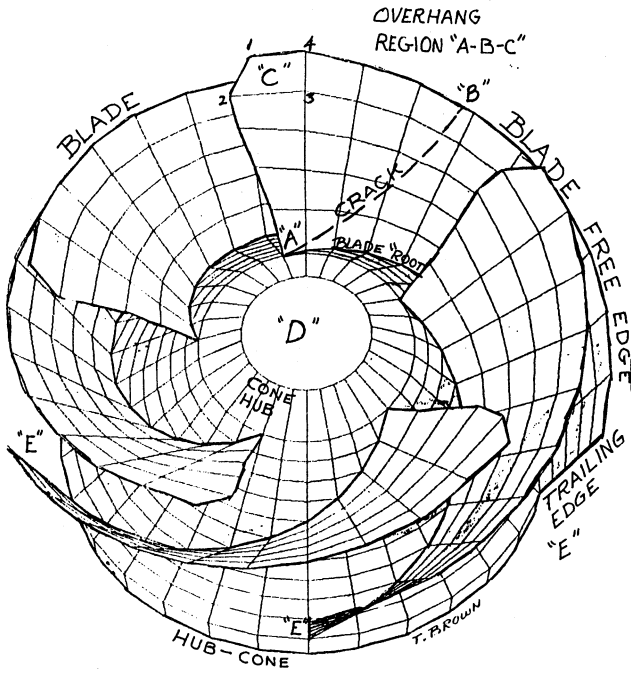


FIG 5. FINITE ELEMENT MODEL OF IMPELLER

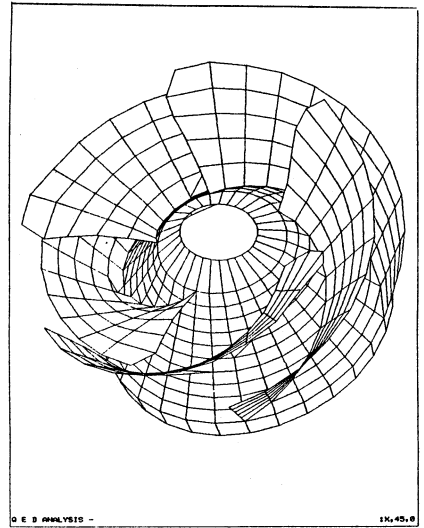


FIG 6. PENDULUM (1st MODE)
OF FIV IN WATER

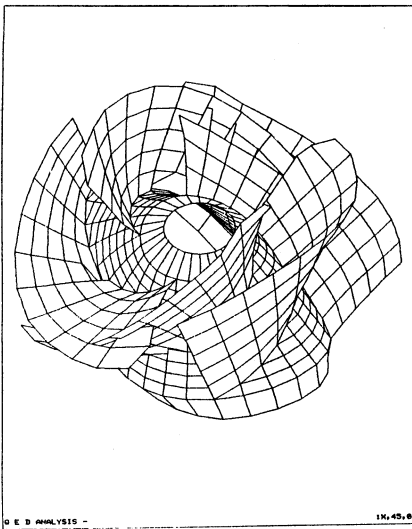


FIG 7. n=2 (2nd MODE)
OF FIV IN WATER

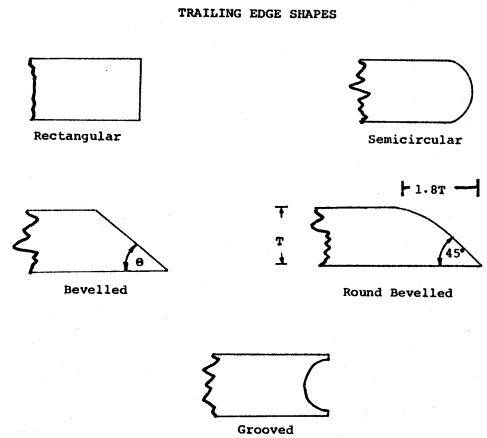


FIG 8. TRAILING EDGE SHAPES